Charged residue changes in the carboxy-terminus of α-tropomyosin alter mouse cardiac muscle contractility

Robert D. Gaffin[1], Kuppan Gokulan[2], James C. Sacchettini[2], Timothy Hewett[3], Raisa Klevitsky[3], Jeffrey Robbins[3] and Mariappan Muthuchamy[1]

[1] *336 Reynolds Medical Building, Cardiovascular Research Institute and Department of Medical Physiology, College of Medicine, Texas A & M University System Health Science Center, College Station, TX 77843-1114, USA*

[2] *Department of Biophysics and Biochemistry, Texas A & M University, College Station, TX 77843, USA*

[3] *Division of Molecular Cardiovascular Biology, Cincinnati Children's Hospital, Cincinnati, OH 45229-3039, USA*

Striated muscle tropomyosin (TM) is an essential thin filament protein that is sterically and allosterically involved in calcium-mediated cardiac contraction. We have previously shown that overexpressing the β-TM isoform in mouse hearts leads to physiological changes in myocardial relaxation and Ca²⁺ handling of myofilaments. Two important charge differences in β-TM compared to α-TM are the exchange of serine and histidine at positions 229 and 276 with glutamic acid and asparagine, respectively, imparting a more negative charge to β-TM relative to α-TM. Our hypothesis is that the net charge at specific sites on TM might be a major determinant of its role in modulating cardiac muscle performance and in regulating Ca²⁺ sensitivity of the myofilaments. To address this, we generated transgenic (TG) double mutation mouse lines (α-TM DM) expressing mutated α-TM at the two residues that differ between α- and β-TM (Ser229Glu + His276Asn). Molecular analyses show 60–88% of the native TM is replaced with α-TM DM in the different TG lines. Work-performing heart analyses show that α-TM DM mouse hearts exhibit decreased rates of pressure development and relaxation ($+\mathrm{d}P/\mathrm{d}t$ and $-\mathrm{d}P/\mathrm{d}t$). Skinned myofibre preparations from the TG hearts indicate a decrease in calcium sensitivity of steady state force. Protein modelling studies show that these two charge alterations in α-TM cause a change in the surface charges of the molecule. Our results provide the first evidence that charge changes at the carboxy-terminal of α-TM alter the functional characteristics of the heart at both the whole organ and myofilament levels.

The sarcomere is a complex array of thin and thick filaments that interact sterically and allosterically to regulate cardiac muscle activation. Tropomyosin (TM), an essential thin filament protein that interacts with actin and troponin (Tn), regulates muscle contraction in a Ca²⁺-dependent manner. Its movement along actin in response to calcium binding to troponin C (TnC) unmasks myosin-binding sites and allows for crossbridge formation.

In vertebrates at least 20 TM isoforms are generated by alternative transcription of the four TM genes (Helfman *et al.* 1986; Ruiz-Opazo & Nadal-Ginard, 1987; Clayton *et al.* 1988; Gunning *et al.* 1990; Lees-Miller *et al.* 1990*a*,*b*) and by alternative splicing (Lees-Miller & Helfman, 1991). Of the four TM genes, only three are cardiac specific: α-TM, β-TM and TPM 3 (Gunning *et al.* 1990; Lees-Miller

& Helfman, 1991; Pieples & Wieczorek, 2000). The α- and β-isoforms have been studied most extensively, and the amino acid sequences share 87% homology. However, differences in the ratios of these isoforms have been noted between fast and slow twitch muscles (Schachat *et al.* 1987), suggesting functional differences.

Although several *in vitro* studies have defined the biological nature of TM, recent transgenic (TG) approaches have explicitly shown that altering the TM isoform population or mutating TM protein in mouse hearts affects cardiac muscle contractility (Muthuchamy *et al.* 1995; Palmiter *et al.* 1996; Prabhakar *et al.* 2001). Normally, the adult mouse heart contains 98% α-TM to 2% β-TM (Muthuchamy *et al.* 1993), but mouse hearts expressing 55% β-TM display diastolic dysfunction,

including increased time to half-relaxation and decreased maximum rates of relaxation (Muthuchamy *et al.* 1995), increased calcium sensitivity in skinned fibre preparations (Palmiter *et al.* 1996), and both decreased maximal rates of contraction and relaxation in isolated cardiomyocytes (Wolska *et al.* 1999). In mouse hearts expressing a very high amount of β-TM (75–80%), death ensued about 10–14 days after birth along with severe cardiac abnormalities including thrombi formation in the atria lumen and the subendocardium of the left ventricle. In addition, physiological analyses using ventricular strips revealed severe contractile and relaxation defects (Muthuchamy *et al.* 1998).

A potential mechanism for the difference in function between these two isoforms is the two charge modifications in β-TM, Ser229Glu and His276Asn, which give it a more negative charge than α-TM. These charge changes could affect its interactions with neighbouring thin filament molecules (McLachlan & Stewart, 1976; Lorenz *et al.* 1995) and may account for weaker binding of fast skeletal β-TM to troponin T (TnT; Thomas & Smillie, 1994). This could effectively cause conformational shifts throughout the troponin complex, thus altering the calcium sensitivity of the myofilaments. Furthermore, charge changes are also responsible for four of the six known TM mutations that cause familial hypertrophic cardiomyopathy (FHC): Lys70Thr (Michele *et al.* 1999), Asp175Asn (Thierfelder *et al.* 1993, 1994), Glu180Gly (Thierfelder *et al.* 1994), and Glu180Val (Regitz-Zagrosek *et al.* 2000). In addition, charge reversals in TM disrupt its association with actin and lead to dilated cardiomyopathy (DCM) in two cases (Glu40Lys and Glu54Lys; Olson *et al.* 2001). Thus, charge changes in TM have great effects on its interactions with other thin filament proteins and are often malevolent. Hence, we hypothesized that the net charge at specific sites on TM might be a major determinant of its role in modulating cardiac muscle performance and in regulating the Ca^{2+} sensitivity of the myofilaments.

To test our hypothesis, we generated TG mice over-expressing mutant α-TM protein in which two of the amino acids at positions 229 and 276 are altered to the corresponding amino acids of β-TM protein, namely Ser229Glu and His276Gln. Results demonstrate that mutant TM protein replaced endogenous TM protein in the sarcomeres and affected cardiac muscle dynamics of contraction and relaxation in work-performing hearts. In addition, skinned papillary bundles from these TG mouse hearts exhibit decreased Ca^{2+}-sensitive force production; however, there is no change in the maximum Ca^{2+}-activated tension. Furthermore, protein kinase A (PKA)-dependent phosphorylation of myofilaments, as occurs

during β-adrenergic stimulation, decreases the Ca^{2+} sensitivity of TG fibres in a manner similar to that seen in control fibres. Protein modelling data suggest that these charge changes in the α-TM alter the surface charge of the molecule and the interaction distance between the monomers of the coiled-coil structure for residues near the charge changes. Thus, our data provide the first evidence that charge modifications at the carboxy-terminus of α-TM modulate the dynamics of muscle contraction and relaxation at the whole heart level and alter the calcium sensitivity in skinned myofilament preparations.

Methods

Generation of the transgenic construct

Site-directed mutagenesis was used to generate mutations at codons 229, TCT to GAG, and 276, CAC to AAC, in α-TM cDNA extracted from mouse hearts. The α-TM mutant cDNA was then ligated to clone 26 which contains the cardiac-specific α-MHC promoter (Subramaniam *et al.* 1991) and the human growth hormone (hgh) polyadenylation (poly A) signal sequence. Mutations were verified by sequencing.

*Bam*H I enzyme was used to release the transgene fragment (7.2 kb) from the pBluescript II vector. The transgene was purified using electroelution and the resulting DNA suspended in 5 mM Tris-HCl, 0.1 mM EDTA, pH 7.4. The purified DNA was microinjected into male pronuclei of fertilized mouse ova for founder mouse generation. These were identified using PCR as described (Walter *et al.* 1989). PCR primers corresponding to nucleotide sequences within the second intron of the MHC promoter and the α-TM cDNA were annealed to genomic DNA from ear clips producing a 234 bp fragment in TG mouse tissue. An additional set of PCR primers, corresponding to nucleotide sequences within the Na^+-K^+ ATPase gene were used as positive controls to verify the presence of intact genomic DNA in both NTG and TG mice. All PCR products were resolved on 1.8% agarose gels. Stable transgenic lines were raised by breeding the founder TG mice with non-transgenic (NTG) cohorts. The generation of transgenic mouse lines and all the experiments using the mouse hearts were approved by the Texas A & M University Animal Care Committee.

S1 nuclease mapping

Total RNA was isolated from both NTG and TG mouse hearts using RNA-Stat 60 (Tel-Test, Friendswood, TX, USA). RNA–DNA hybridization, followed by S1 nuclease analyses, was conducted under conditions previously

described (Wieczorek *et al.* 1985). To distinguish α-TM 229 transcripts from endogenous α-TM mRNAs, a PCR probe that incorporates the second and third exon of α-MHC (15 bp) and 262 nucleotides of the α-TM coding region was utilized. In S1 nuclease mapping analyses, this probe protects 262 nucleotides of endogenous α-TM, whereas a 277 bp fragment is protected for mutant α-TM transcripts. A control GAPDH probe was used for quantitative purposes.

DNA probes for the hybridization reaction were created using PCR. Single-stranded DNA probes used for hybridization were labelled at the 3′-end with γ-^{32}P adenosine triphosphate (Amersham) via T4 kinase (Invitrogen). The sequences for the S1 probes were as follows: 5′-TM primer, 5′-GCCCACACCAGAAATGACAGACAG-3′; 3′-TM primer, 5′-GAGAAGCTACGTCAGCTTCAGCAT-3′; glyceraldehyde-3-phosphate dehydrogenase probe was also prepared via PCR. Hybridized RNA–DNA strands were electrophoresed on 6% polyacrylamide gels (19 : 1) containing 8.3 M urea. Gels were dried and auto-radiographed on Kodak X-Omat AR film. Densitometry analysis of the resulting bands using Multi-Analyst software (Bio-Rad) and phosphorimaging analyses were conducted to determine RNA content. Quantification was performed using the volume integration method with subtraction of the tRNA control lane as background. Three separate RNA gels were used to quantify the relative levels of transcripts.

Gel electrophoresis and Western blotting

SDS-polyacrylamide gel electrophoresis was performed according to the method of Laemmli (Laemmli, 1970). Modified procedures from Pagani & Solaro (1984) were used to isolate myofibrils from the heart with all solutions being supplemented with 1 μg μl^{-1} leupeptin and 1 mM phenylmethylsulphonyl fluoride. Protein concentrations for each sample were determined using the BCA protein estimation kit (Pierce). Protein (7.5 μg) was separated on a 10% SDS gel containing 3.4 M urea (Schachat *et al.* 1985) and transferred to a nitrocellulose membrane according to the method of Towbin *et al.* (1979) for Western blot analysis. Primary antibody incubations in 5% non-fat milk were performed with a 1 : 40 000 dilution of CH-1 antibody (from a 1.5 mg ml^{-1} stock; Developmental Studies Hybridoma Bank, University of Iowa) that recognizes both endogenous and mutant forms of tropomyosin. Secondary antibody incubations were performed with goat anti-mouse IgG conjugated to horseradish peroxidase (1 : 80 000; Sigma). Chemiluminescence (SuperSignal West Pico; Pierce) was used as the detection agent.

Densitometry on the resulting bands were performed using Multi-Analyst software.

To verify equal loading of each sample, membranes were stripped using ImmunoPure IgG elution buffer (Pierce) and then re-probed with antisarcomeric actin primary antibody (1 : 5000 dilution; Sigma) followed by goat anti-mouse IgM (1 : 10 000 from a 0.6 mg ml^{-1} stock; Sigma) as the secondary antibody. The resulting TM/actin ratio was used as an indicator of equal loading. Chemiluminescence (SuperSignal, WestPico) was again used as the detection agent. Western blot analysis of myo-fibrillar proteins followed by quantification was performed three times for each sample and the resulting mean values ± s.e.m. calculated.

Physiological measurements of left ventricular function

The isolated working heart preparations have been described (Gulick *et al.* 1997). Briefly, age-matched male mice (4–6 months) were anesthetized with sodium pento-barbital (30 mg kg^{-1}, i.p.) and the hearts immediately excised. A 20 gauge cannula was tied onto the aortic stump to allow the regulation and recording of mean arterial pressure (MAP) and aortic flow (Transonic Flow Probe Model T206; Transonic Systems Inc., Ithaca, NY, USA). A silastic fluid-filled catheter was inserted through the apex of the left ventricle to record intraventricular pressure. Left ventricular pressure was measured as systolic, diastolic and end-diastolic pressure using the DigiMed systems analysers BPA-2000, HPA-200, HPA-210 and LPA-200 (Micro-Medical, Inc., Louisville, KY, USA). The fluid-filled catheter system responded well within experimental requirements without distortion up to a frequency of 600 beats min^{-1}. A 20 gauge cannula was tied into the left pulmonary vein to accommodate regulation on recording of venous return (cardiac output). The catheter was completely water-jacketed for improved temperature (37.4°C) regulation of the Krebs-Henseleit solution that was returned to the left side of the heart for anterograde perfusion. Custom-designed software calculated heart rate, MAP, left ventricular pressure, peak systolic pressure, time to peak pressure, half-time of relaxation, the first derivatives of the change in left ventricular systolic pressure with respect to time ($\pm dP/dt$), left atrial pressure, and perfusate temperature. The arterial P_{O_2} was 650 mmHg and the $P_{CO_2} \sim 30$ mmHg. The data are expressed as mean ± s.e.m. Starling curves were generated by linear regression using Statview version 5.01 (Abacus Concepts Inc., Berkeley, CA, USA).

Skinned fibre preparations

Adult mice (3–4 months old; 25–35 g) were anaesthetized with sodium pentobarbital (150 mg (kg body weight)$^{-1}$, I.M.) and the hearts quickly removed and put into high-relaxing solution of the following composition (mM): KCl 53.3, EGTA 10, MOPS 20, free MgCl$_2$ 1, MgATP 5.4, creatine phosphate 12. The pH of the solution was adjusted to 7.0 with KOH. Papillary muscles from the left ventricle were dissected, and small fibre bundles ∼150–250 μm in width and 2–3 mm in length were prepared. The fibre bundles were mounted between clips on a micromanipulator and a force transducer. Fibres were skinned for 30 min in high-relaxing solution containing 1% Triton X-100. After skinning, the fibres were initially washed with high-relaxing solution and then sequentially bathed in low-relaxing solution. Compared to high-relaxing solution, low-relaxing solution contains 0.1 mM EGTA. A resting sarcomere length of 2.2 μm was then established from laser diffraction patterns (Hibberd & Jewell, 1982). Isometric tension was recorded on a digital phosphor oscilloscope suite (Tektronix TDS 3014 with Wavestar software, Tektronix) after development in solutions of varying pCa values. All solutions contained the protease inhibitors pepstatin A (2.5 μg ml^{-1}), leupeptin (1 μg ml^{-1}) and phenylmethylsulphonylfluoride (PMSF; 50 μM).

After initial Ca^{2+}–force relationships were established, cAMP-dependent phosphorylation of skinned fibres was induced by incubation in low-relaxing solution containing 100 μM cAMP + 100 ng ml^{-1} calyculin A for 30 min (Palmiter *et al.* 1996). Force development was again recorded using similar solutions with the addition of 100 μM cAMP + 100 ng ml^{-1} calyculin A. Results are presented as mean ± S.E.M. The force–pCa relation was fitted to the Hill equation with non-linear analysis to derive the pCa$_{50}$ (calcium concentration at 50% of maximum force) and Hill coefficient using Prism software (Graphpad). Shifts in the pCa$_{50}$ value and the Hill coefficient were analysed using Student's unpaired *t* test, significance set at $P < 0.05$.

Protein modelling

Atomic coordinates for the full length of TM are available from the RCSB Protein Data Bank at www.rcsb.org/pdb (PDB ID code 1C1G; Whitby & Phillips, 2000). The pdb coordinates were read in the Xtalview (McRee, 1999), and point mutations were made at positions 229 and 276. The GRASP program (Nicholls *et al.* 1991) was used to perform electrostatic analyses and surface rendering of TM. To calculate the distance between the C-α carbon atom and carbonyl atom of the two strands of TM, we minimized the mutant structure in the Insight II suite, using Discovery (Accelrys).

Results

The generation of mutant α-TM DM mice α-TM cDNA was subjected to site-directed mutagenesis to generate TCT to GAG and CAC to AAC transitions at codons 229 and 276, respectively. This resulted in Ser→Glu and His→Asn amino acids changes at 229 and 276 positions of α-TM. The α-TM double-mutated (α-TM DM) cDNA was then inserted into clone 26 at *Sal* I and *Hin*d III sites, which contains the cardiac-specific α-MHC promoter. The 3′ end was ligated to human growth hormone (hgh), a poly-adenylation/termination sequence (Fig. 1*A*), which helps ensure that the mutant transcript is processed correctly. The sequence was then isolated from its vector, purified via electrophoresis, and injected into male pronuclei to produce founder TG mice. Germ-line transmission of the transgene was confirmed by PCR analysis of DNA from mice ear clips. Southern blot analysis was conducted to verify the presence of the 7.2 kb transgene within the genomic DNA of transgenic mice (data not shown). None of the founder mice or their progeny demonstrated any gross phenotypic alterations or reduced viability.

Replacement of α-TM with α-TM DM protein in hearts of TG mice

Previous studies from our laboratory have shown that mice overexpressing β-TM or mutant α-TM in the heart have a concomitant decrease in endogenous α-TM; however, the amount of total cardiac TM remains equal to the levels seen in NTG hearts (Muthuchamy *et al.* 1995, 1999). We wished to ascertain whether this same phenomenon occurred in the α-TM DM TG mice. Thus, we analysed both endogenous and mutant RNA and protein levels in α-TM DM hearts. S1 nuclease protection assays were conducted to determine the relative levels of endogenous *versus* mutant TM mRNA. GAPDH transcript levels were used as a control in quantification. In this assay, 20 μg of RNA from both NTG and TG hearts was hybridized to two radioactively labelled probes, TM and GAPDH control. Hybridized products were then subjected to digestion by S1 nuclease and analysed as described (Muthuchamy *et al.* 1993). As shown in Fig. 1*B*, the 320 nucleotides probe can distinguish between endogenous TM mRNA (262 nt) and α-TM DM mRNA (277 nt). The band corresponding to α-TM DM can be seen in all TG heart RNA samples. Note the concomitant decrease in endogenous TM RNA levels when compared to levels in NTG mice. Thus, a compensatory mechanism exists at the molecular level that regulates TM

levels in α-TM DM mice, consistent with our previous overexpression studies (Muthuchamy *et al.* 1995, 1999). Quantitative phosphorimaging and densitometry analyses demonstrate that 89.2% mutant α-TM DM message is present in TG line DM-A. DM-5 and DM-13 TG lines have 56.6% and 49.9% mutant transcripts, respectively (Fig. 1*C*).

To examine the effects of α-TM DM transgene expression on the myofilament protein profile, we analysed myofibrillar protein fractions of both TG and NTG hearts. SDS-PAGE gels containing 3.4 M urea (Schachat *et al.* 1985) effectively separate endogenous TM from α-TM

DM protein (Fig. 2*A*). Western blot analyses of these gels (Fig. 2*B*) show that NTG samples contain only one TM species while the TG samples show two bands, the slower migrating α-TM DM and the endogenous TM protein. The reason for the slower migration of the α-TM DM may be due to charge changes resulting from the mutations at residues 229 and 276. Ser229Glu creates an additional negative charge in the structure and His276Asn removes a positive charge from α-TM. The net effect is a gain of two negative charges in α-TM DM when compared to native α-TM. However, it should be noted that these endogenous and mutant α-TM bands were unable to be resolved in
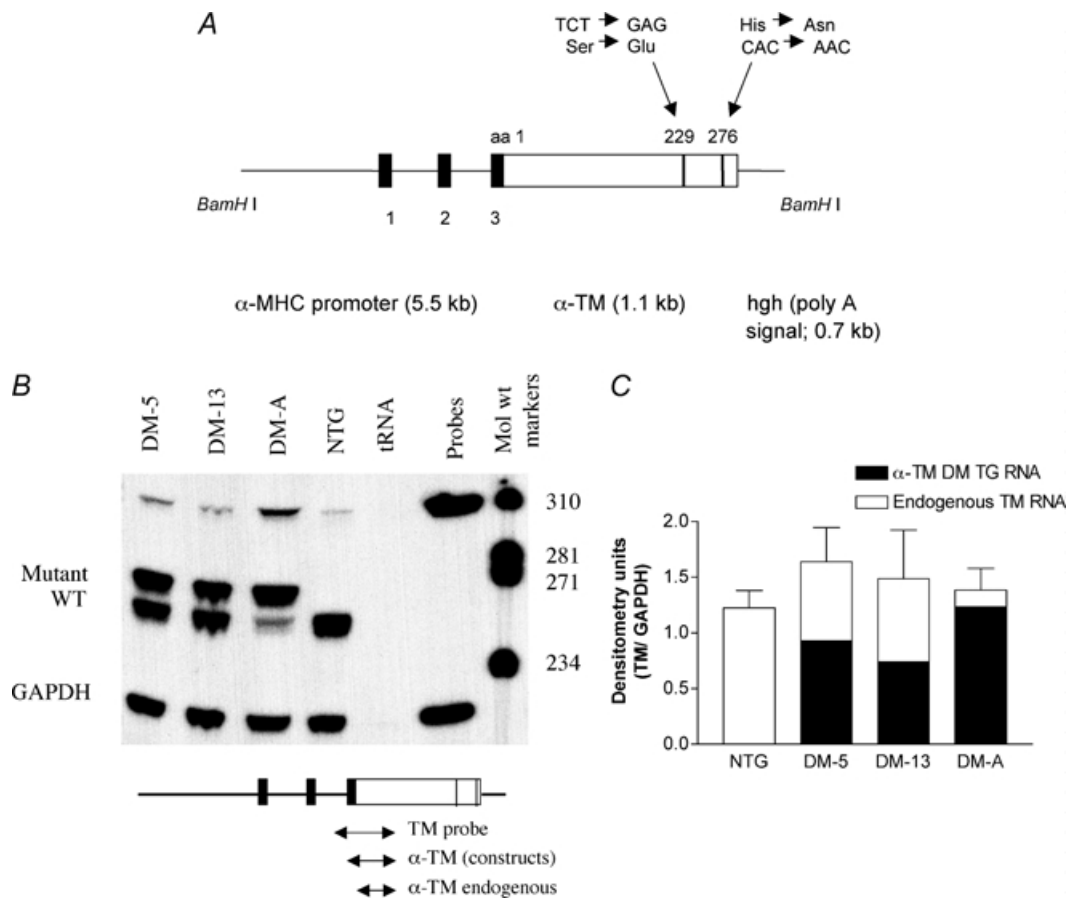

Figure 1. α-TM DM construct and mRNA expression
A, schematic representation of the TG construct. The mutant TM (Ser229Glu + His276Asn) was linked to the α-MHC promoter (Subramaniam *et al.* 1991) and used to generate multiple lines of TG mice. The human growth hormone polyadenylation site (hgh poly A) was placed downstream of the TM cDNA. The filled boxes denote the exons derived from α-MHC that encode the 5′-untranslated region. The construct was released using *Bam*H I enzyme. *B*, RNA expression in TG mice. Total cardiac RNA (20 μg) was hybridized to 3′-radioactively labelled DNA probes specific for either TM (see the small diagram below the RNA gel) or GAPDH. TM probe is 320 bp in length and yields fragments of 277 bp for α-TM DM and 262 bp for endogenous TM RNA after S1 nuclease treatment. The electrophoresed samples shown here contain both mutant and endogenous bands for α-TM DM samples and an endogenous band only for NTG hearts. tRNA was used as a negative control. *C*, quantification of RNA. NTG and α-TM DM RNA levels were quantified on a PhosphorImager and via densitometry using Bio-Rad's Multi-Analyst software. All three TG lines showed some degree of α-TM DM expression; however, the DM-A line expressed more TG RNA compared with the other two lines.

SDS-PAGE without urea (data not shown), whereas the α- and β-TM bands can be resolved using SDS-PAGE (Muthuchamy *et al.* 1995; Palmiter *et al.* 1996; Wolska *et al.* 1999). The DM-A transgenic line expresses higher levels of mutant protein (88.0%) compared with that of DM-5 or DM-13 TG lines (73.0 and 59.0%, respectively; Fig. 2*C*). These results corroborate well with the RNA data.

The α-TM DM hearts are hypodynamic

In order to determine the functional properties of α-TM DM hearts, isolated cardiac function in the absence of neurohumoral input was assessed using work-performing isolated heart preparations in age-matched, male NTG and α-TM DM (DM-A) hearts. The results indicated that α-TM DM hearts were hypodynamic and possibly failing compared to their NTG littermates as evidenced by the high rate of preparation failure (4 of 6 α-TM DM hearts failed during testing as opposed to only 1 of 6 NTG hearts). The α-TM DM TG mouse hearts exhibited a significantly lower rate of ventricular tension development ($+dP/dt$) and significantly reduced kinetics of cardiac relaxation ($-dP/dt$) compared to NTG hearts (Fig. 3 and Table 1). Other contractile and relaxation parameters such as time to peak pressure and τ (index of relaxation; time from peak pressure to the tangent line of the steepest rate of pressure fall) are also significantly altered in the TG mouse hearts.
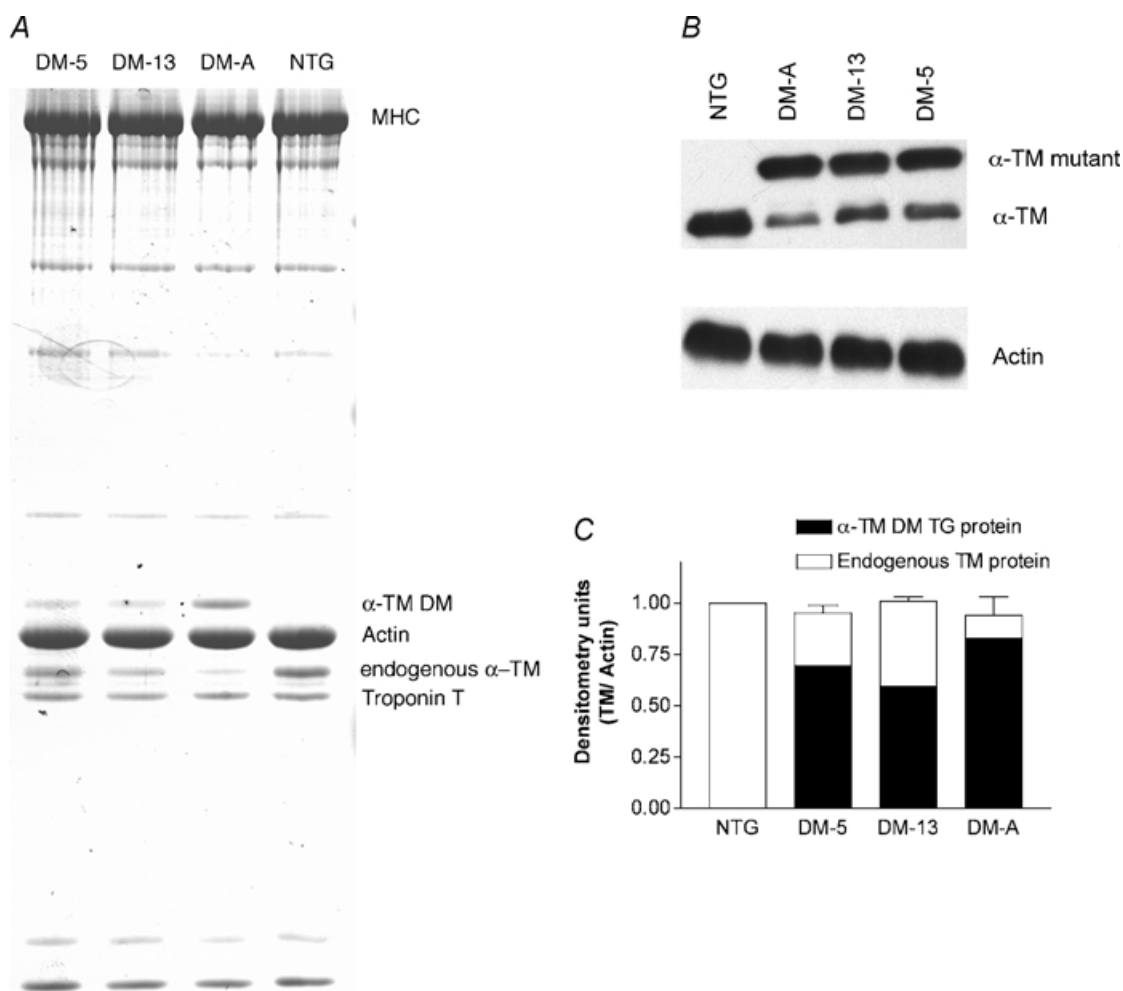

Figure 2. Protein expression in α-TM DM mice
A, 8 μg of total cardiac myofibrillar proteins from NTG or TG mice were electrophoresed on SDS-PAGE gels containing 3.4 M urea and stained with Coomassie blue. *B*, Western blot of total myofibrillar proteins electrophoresed on SDS-PAGE gels containing 3.4 M urea. Nitrocellulose filters were first probed with a striated muscle-specific antibody, CH-1, then stripped and reprobed with a sarcomeric actin-specific antibody to verify equal loading for each sample. Note that TG samples contain both α-TM DM and endogenous TM while the NTG sample contains only endogenous TM. *C*, densitometric analysis of Western blots shown in *B*. In each sample, total α-TM DM plus endogenous TM was divided by actin amounts and results normalized to NTG. Note that total TM levels were similar for NTG and TG samples.

These results demonstrate that the cardiac performance of α-TM DM hearts is altered drastically by TG expression, resulting in diminished rates of both contraction and relaxation.

To further determine the mechanisms for this decreased rate of contraction and relaxation in the TG mouse hearts, we measured isometric force in myofilaments prepared from NTG and α-TM DM TG mouse hearts (Fig. 4). The force generated by α-TM DM TG myofilaments was less sensitive to Ca^{2+} when compared with NTG myofilaments (Fig. 4A). The pCa_{50} for NTG preparations was 5.83 ± 0.02 and 5.75 ± 0.02 ($n = 8$ from 4 different hearts; $P < 0.01$) for α-TM DM myofilament preparations. In addition, myofilaments from α-TM DM TG mouse hearts showed a slight, albeit non-significant, increase in cooperativity when compared to NTG preparations. The Hill coefficient was 3.40 ± 0.18 in NTG and 3.84 ± 0.34 ($P > 0.05$) in TG hearts. Figure 4B shows the relationship between average active tension and pCa in NTG and TG myofilament preparations. There is no significant change in the maximum force in the TG group compared to NTG controls. However, the force of fibre bundles prepared from TG hearts is less sensitive to Ca^{2+}, as seen in Fig. 4A. In order to assess the function of troponin I (TnI) in α-TM DM TG mice, we also incubated skinned fibre bundles with 100 μM cAMP and 100 ng ml^{-1} calyculin A, a phosphatase inhibitor. This treatment mimics the effects of PKA-mediated phosphorylation during β_1 adrenergic stimulation. NTG fibres display a characteristic decrease in Ca^{2+} sensitivity upon phosphorylation of TnI by PKA (Guo *et al.* 1994; Palmiter *et al.* 1996). The fibre bundles from α-TM DM TG mouse hearts also display a rightward shift in Ca^{2+} sensitivity (Fig. 4C). The pCa value for NTG myofilament preparations treated with cAMP was 5.75 ± 0.01, and 5.64 ± 0.02 ($n = 8$ from 4 different hearts) for α-TM DM TG preparations. The Hill coefficient after cAMP treatment was 3.10 ± 0.24 in NTG and 3.92 ± 0.31 in TG hearts ($P > 0.05$). Thus, the decrease in Ca^{2+} sensitivity in response to TnI phosphorylation is maintained in the TG preparations when compared with NTG samples.

α-TM DM hearts are not morphologically different from NTG hearts

Histological analyses showed no evidence of anomalies in chamber dimension, fibrosis, inflammation or hypertrophy in α-TM DM mice when compared to NTG mice. Heart weight to body weight ratios indicate a slight increase in α-TM DM mice (4.22 ± 0.067 for NTG, $n = 26$, *versus* 4.65 ± 0.085 for α-TM DM, $n = 10$; $P < 0.005$), but there were no changes in the mortality rates for α-TM DM mice and no obvious phenotypic changes could be detected.

Surface charges are altered in the α-TM DM protein

To further investigate the effects of charge changes on α-TM protein structure, we performed predicted surface charge analyses on α-TM and α-TM DM proteins as described in Methods. In the native TM molecule the surface charge is predominately negative, which is depicted in Fig. 5A as red colour on the molecule surface. Figure 5B shows that the two mutations in α-TM cause a local change in electrostatic potential near residue 229. It is clearly seen in Fig. 5B that the change from serine to glutamic acid at position 229 brings an increase of negative charge potential (more red colour) in this region of the molecule.

In addition, we measured the distance between the Cα carbon atoms and carbonyl atoms (near the mutated regions) of the two-monomer strands for both normal and mutant TM molecules as described in Methods. In the normal TM structure, the distance between the Cα carbon atoms of the two strands at residues 229, 230 and 231 is 9.2, 14.2 and 10.1Å; whereas, in the mutant molecule, the distances are 9.32, 14.38 and 11.01Å, respectively. The distance between the carbonyl atoms at these residues are the following: in the normal structure, 10.7, 12.6 and 7.89Å; in the mutant molecule, 11.12, 13.05 and 8.2Å, respectively. Near the 276 region, the estimated values between the Cα carbon atoms of the two strands at residues 275, 276 and 277 in the normal TM are 12.87, 13.36 and 6.15Å; in the mutant molecule, they

Figure 3. Physiological analyses of left ventricular function

Contractile parameters in NTG and α-TM DM TG mouse hearts were compared. Baseline values were set at 5 ml min^{-1} cardiac output and 50 mmHg mean aortic pressure. Other conditions are described in Methods. Rates of contraction ($+dP/dt$) and relaxation ($-dP/dt$) are significantly reduced in the TG mouse hearts. $***P \leq 0.001$
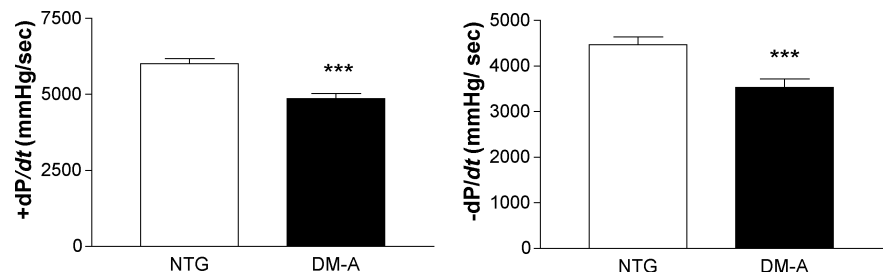
Table 1. Measured haemodynamic parameters of non-transgenic (NTG) and α-TM DM transgenic (TG) hearts

	NTG male hearts	TM DM male hearts	Percentage change *versus* NTG
Working heart	($N = 5, 50$)	($N = 2, 20$)	
Heart rate (beats min^{-1})	405 ± 1	404 ± 1	Paced n.s.
+dP/dt (mmHg s^{-1})	6014 ± 167	4863 ± 170	-19**
−dP/dt (mmHg s^{-1})	4469 ± 170	3530 ± 186	-21**
LVP (mmHg)	109 ± 3	105 ± 2	n.s.
Time to peak pressure (ms)	46 ± 1	42 ± 1	-9*
τ	20 ± 1	27 ± 7	$+35$*

Values are mean $\pm$ S.E.M. *$P \leq 0.05$, **$P \leq 0.001$, transgenic *versus* control, Student's unpaired t test. LVP, left ventricular pressure; N; number of mouse hearts.

are 13.17, 13.65 and 6.30Å, respectively. The carbonyl atoms distance at residues 275, 276 and 277 is 12.92, 11.19 and 6.2Å in the normal *versus* 13.33, 11.07 and 6.53Å in the mutant molecule. Thus, these two mutations cause a significant change (0.3–0.9Å) in the distance between the monomer strands in localized regions of α-TM. These changes, in turn, could affect the interactions of α-TM with neighbouring thin filament molecules such as actin and TnT.

Discussion

The data presented here show that charge changes in the carboxyl end of α-TM alter the structure and function of TM. In mice containing nearly 90% replacement (line A) of endogenous α-TM with α-TM DM, hearts were hypodynamic as evidenced by a decrease in +dP/dt and −dP/dt when compared to NTG mice. In fact, only 33% of the isolated TG mouse hearts were able to survive the transition from the Langendorff perfusion to the working heart preparation. Thus, in the absence of neurohumoral stimuli, the TG hearts expressing higher levels of mutant protein appear to be failing, although *in vivo*, there were no obvious differences in mortality rates between the TG mice and NTGs. The depression in the rate of contractility can be attributed to a decrease in Ca^{2+} sensitivity, which is corroborated by our skinned fibre data. The attenuation in the rate of relaxation could be explained by the slight increase in cooperativity seen in the α-TM DM myofilaments, which may also affect the kinetics of relaxation, or the constant 'g' as described by Campbell (Campbell, 1997). The increase in the cooperativity mechanism would also be expected to slow the rate of force development (Campbell, 1997; Moss, 1999). Future studies comparing the kinetics of force development in skinned preparations

from NTG and TM DM TG hearts will further elucidate the mechanisms of reduced cardiac performance in these TG mouse hearts.

TM protein is a highly charged molecule that is believed to interact with actin by ionic interactions, most likely via Mg^{2+} salt bridges between negatively charged residues on either molecule (McLachlan & Stewart, 1976). Murine striated α-TM has 80 acidic residues (aspartic acid, 24; glutamic acid, 56) and 55 basic amino acid residues (histidine, 2; lysine, 39; arginine 14). Thus, the net charge of the TM molecule is negative, and the two residues that we altered, 229 and 276, would further increase the negative charge of TM. Protein modelling data clearly demonstrate that these charge alterations in α-TM alter the surface charge potential of the molecule in localized regions. Also, the distance between the two monomer strands of the molecule are altered, implicating that these changes in the mutant TM protein would affect the interactions of mutant TM with its neighbouring molecules, specifically troponin T and actin, thereby altering cardiac muscle dynamics.

A consideration for the detrimental cardiac effects of a charge change mutation at residue 229 is its location in a region of TM (residues 143–235) that has been described as unstable for two reasons (Paulucci *et al.* 2002). First, this region contains a charged residue, Glu218, which occupies one of the normally hydrophobic core positions, *a*, of TM's heptad repeat (*a, b, c, d, e, f, g*) (McLachlan & Stewart, 1975). Second, this region also contains two interacting negatively charged residues that occupy the *g* (Asp175) and ($n + 5$) *e'* (Glu180) position of TM's heptad repeat. Normally, the *e* position is occupied by a negatively charged acidic residue while the *g* position is occupied by a positively charged basic residue or a polar residue (Smillie, 1996). This interaction promotes favourable salt bridges that add stability to TM's coiled coil. In this case, both residues are negatively charged creating a repulsion, which adds instability to this region of TM. Altering residue 229 from Ser to Glu would create a similar repulsion since residue 229 occupies an *e'* position and Glu224 occupies the corresponding *g* position. This repulsion could then cause conformational strains in that region of the TM. Taken together we predict that the Ser229Glu mutation causes further instability in the 143–235 region of TM.

Another consideration for the effects of a charge change at residue 229 is its proximity to the sixth alanine cluster as proposed by Brown *et al.* (2001). The seven alanine clusters in TM's helical structure (Brown *et al.* 2001) impart conformational bends and yield flexibility to TM's coiled-coil design, thus allowing more effective interaction with actin. Residue 229 lies close to the sixth

alanine cluster and residue 276 lies adjacent to Ala277, the seventh cluster. Charge changes in these two residues would have repercussions on nearby amino acid side chains, as indicated in our structural data, and thus could alter the conformational bends in TM imparted by these two alanine clusters.

In addition, residue 229 lies in a positive zone of a β-band in TM's 14-fold repeat of actin interaction sites (McLachlan & Stewart, 1976). The β-band has been implicated in the 'on' state of myofilament activation, and the positive zones are primarily filled with hydrophobic residues allowing for close contact between TM and actin. Adding a negative charge in this region, along with its adjacent neighbour Asp230, which is also negatively charged, would diminish non-polar interactions thus creating weaker binding in the 'on' state.

Residue 276 is also a critical residue as it lies in the overlap region for contiguous TM molecules and in the region of TM–TnT interaction. Thus, a charge change in this residue confers conformational changes that affect TM's interactions with the troponin complex and neighbouring TM molecules. Altered TM–TnT interactions could adversely affect movement of the troponin complex in the modified three-state model of allosteric activation (Squire & Morris, 1998), which could negatively impact force generation. Furthermore, Hitchcock-DeGregori's group have shown that the carboxy-terminus end of TM is responsible for actin affinity, which is the primary factor
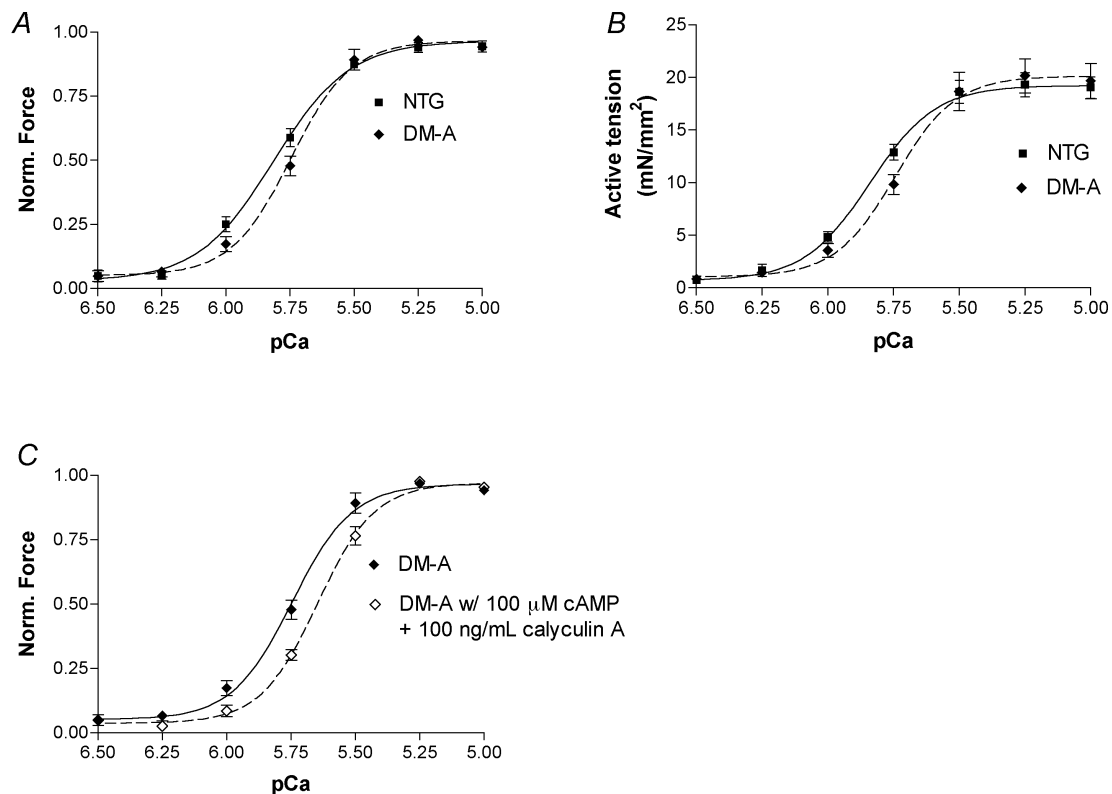

Figure 4. Ca^{2+}–force relationships in skinned fibre papillary bundles from NTG and α-TM DM mouse hearts

A, force was normalized to the corresponding maximum force at pCa 4.5. Data are presented as mean ± S.E.M. pCa$_{50}$ for NTG fibres (filled squares; continuous line) was 5.83 ± 0.02 and cooperativity was 3.40 ± 0.18; pCa$_{50}$ for α-TM DM fibres (filled diamonds; dashed line) was 5.75 ± 0.02 and cooperativity was 3.84 ± 0.34. $n = 8$ from 4 different hearts for both NTG and TG. Other conditions are described in Methods. *B*, pCa *versus* active tension (mN mm^{-2}). Data are presented as mean ± S.E.M. There was no significant change in active tension between NTG (filled squares; continuous line) and α-TM DM (filled diamonds; dashed line) fibre preparations. *C*, normalized pCa–force relation in skinned fibre preparations from α-TM DM mouse hearts before and after cAMP treatment. Data are presented as mean ± S.E.M. Note the rightward shift after cAMP movement. pCa$_{50}$ for α-TM DM fibres after cAMP treatment (open diamonds; dashed line) was 5.64 ± 0.02 and cooperativity was 3.92 ± 0.31. Other experimental conditions are described in Methods.

by which myosin S1 induces TM binding to actin in the open state (Hammell & Hitchcock-DeGregori, 1996; Moraczewska *et al.* 1999; Moraczewska & Hitchcock-DeGregori, 2000). The effects of this on force production are unknown, but our data suggest that a charge change in that region of TM affects both contraction and relaxation in isolated hearts and calcium sensitivity in detergent-extracted fibres.

Finally, the Ser229Glu and His276Asn changes in the α-TM molecule altered the net charge similar to the β-TM molecule. Initially we expected that these changes in the α-TM might have altered the α-TM DM TG mouse heart function similar to β-TM TG mouse hearts (Muthuchamy *et al.* 1995; Palmiter *et al.* 1996). However, our data show that the α-TM DM TG mice do not possess the same cardiac performance profile as the β-TM TG mice. Specifically, α-TM DM mouse hearts (which express 88% of mutant protein) exhibit a decrease in both contractile as well as relaxation parameters, and calcium sensitivity of the myofilaments is decreased in these mice. Yet, in the β-TM TG studies, replacement of 55% of endogenous α-TM by β-TM proteins in the TG heart resulted in a decreased rate of relaxation in working-heart preparations and an increase in calcium sensitivity in skinned-fibre studies (Muthuchamy *et al.* 1995; Palmiter *et al.* 1996). However, in TG mouse hearts expressing higher levels of β-TM (75% β-TM and 25% α-TM), there were significant depressions in both contractile and relaxation parameters that eventually led to lethality in these animals (Muthuchamy *et al.* 1998). Thus, we conclude that the stoichiometric ratios of wild-type (α-TM) to TG (β-TM) play a role in determining the difference in cardiac performance resulting from α- or β-TM expression. Since α-TM DM mimics the charge of β-TM, it seems reasonable that the high expression (88%) in α-TM DM TG mice would have a cardiac performance profile similar to β-TM TG hearts expressing higher levels of β-TM protein. This is consistent with the data we present here excluding the increase in mortality rate for high-expression β-TM TG mice.

Other amino acid incongruities, besides the difference in charged residues, may also play a role in determining the variations in cardiac performance between β-TM TG mice and α-TM DM TG mice. For example, the C-terminal region of TM, where TM–TnT interaction and TM–TM overlap occur, contains 25 of the 39 amino acids that differ between α-TM and β-TM. This region contains the
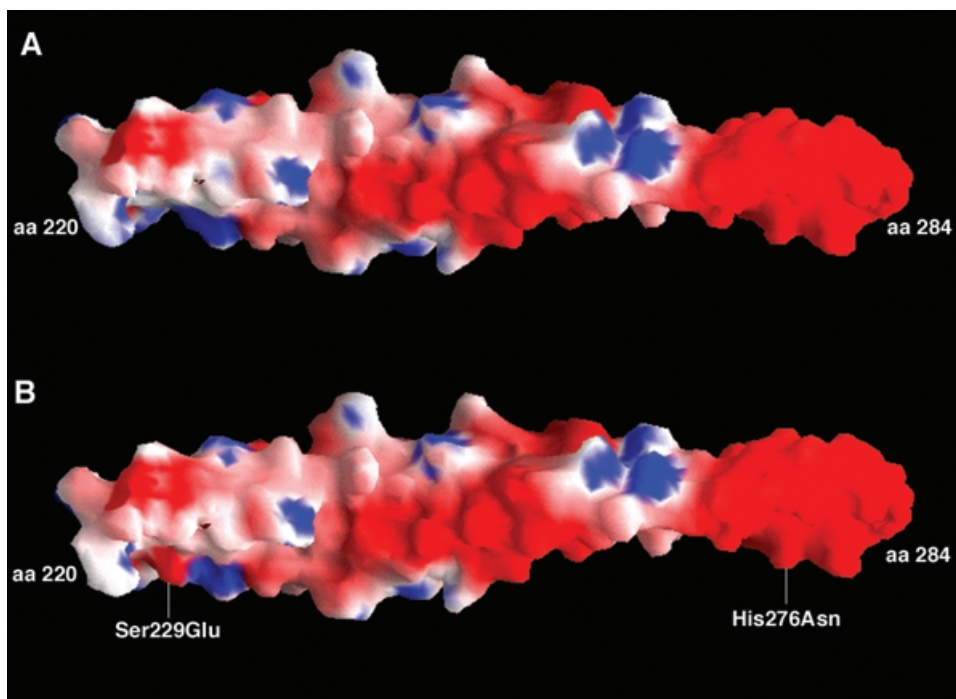

Figure 5. Electrostatic surface models of native and mutant TMs
A, native α-TM. *B*, α-TM DM. The molecular surface is coloured by electrostatic potential (red, $-9.8kT/e$; white, neutral; blue, $+3.4kT/e$). The mutation site is marked. The C-terminal residues (220–284) of TM were included in the analyses whereas the N-terminal residues (1–219) were omitted for simplicity.

two sites of TnT–TM interaction including the variable ninth exon. A recent study by Jagatheesan *et al.* (2003), in which the terminal, ninth exon (9a) is replaced with its β-TM counterpart, also showed depressed contractile (+dP/dt) and lusitropic (−dP/dt) parameters in whole heart preparations and decreased calcium sensitivity in skinned fibre preparations of TG mouse hearts. These phenotypes are similar to the α-TM DM mouse hearts but quite different from the β-TM TG mouse hearts. Thus, the difference in function between α-TM and β-TM could be the combination of several amino acid differences between the two isoforms, not just the charge changes.

In summary, charge changes in α-TM affect cardiac function. It is well established that charged residues within the TM sequence are important, such as those which compose the 14-fold repeat of acidic and polar residues implicated in binding actin in the 'on' and 'off' states of muscle contraction (Parry, 1975; Stewart & McLachlan, 1975; McLachlan & Stewart, 1976). Charge changes within TM are also responsible for FHC (Thierfelder *et al.* 1993, 1994; Michele *et al.* 1999; Regitz-Zagrosek *et al.* 2000) and DCM (Olson *et al.* 2001) in several cases. Our data suggest that charge changes at residues 229 and 276 play an important role in the structure and function of striated α-TM. More research on the charged surface residues of α-TM is needed to give further insights in understanding cardiac muscle regulation.

References

Brown JH, Kim KH, Jun G, Greenfield NJ, Dominguez R, Volkmann N, Hitchcock-DeGregori SE & Cohen C (2001). Deciphering the design of the tropomyosin molecule. *Proc Natl Acad Sci U S A* **98**, 8496–8501.

Campbell K (1997). Rate constant of muscle force redevelopment reflects cooperative activation as well as cross-bridge kinetics. *Biophys J* **72**, 254–262.

Clayton L, Reinach FC, Chumbley GM & MacLeod AR (1988). Organization of the hTMnm gene. Implications for the evolution of muscle and non-muscle tropomyosins. *J Mol Biol* **201**, 507–515.

Gulick J, Hewett TE, Klevitsky R, Buck SH, Moss RL & Robbins J (1997). Transgenic remodeling of the regulatory myosin light chains in the mammalian heart. *Circ Res* **80**, 655–664.

Gunning P, Gordon M, Wade R, Gahlmann R, Lin CS & Hardeman E (1990). Differential control of tropomyosin mRNA levels during myogenesis suggests the existence of an isoform competition-autoregulatory compensation control mechanism. *Dev Biol* **138**, 443–453.

Guo X, Wattanapermpool J, Palmiter KA, Murphy AM & Solaro RJ (1994). Mutagenesis of cardiac troponin I. Role of the unique NH$_2$-terminal peptide in myofilament activation. *J Biol Chem* **269**, 15210–15216.

Hammell RL & Hitchcock-DeGregori SE (1996). Mapping the functional domains within the carboxyl terminus of alpha-tropomyosin encoded by the alternatively spliced ninth exon. *J Biol Chem* **271**, 4236–4242.

Helfman DM, Cheley S, Kuismanen E, Finn LA & Yamawaki-Kataoka Y (1986). Nonmuscle and muscle tropomyosin isoforms are expressed from a single gene by alternative RNA splicing and polyadenylation. *Mol Cell Biol* **6**, 3582–3595.

Hibberd MG & Jewell BR (1982). Calcium- and length-dependent force production in rat ventricular muscle. *J Physiol* **329**, 527–540.

Jagatheesan G, Rajan S, Petrashevskaya N, Schwartz A, Boivin G, Vahebi S, DeTombe P, Solaro RJ, Labitzke E, Hilliard G & Wieczorek DF (2003). Functional importance of the C-terminal region of striated muscle tropomyosin. *J Biol Chem* **278**, 23204–23211.

Laemmli UK (1970). Cleavage of structural proteins during the assembly of the head of bacteriophage T4. *Nature* **227**, 680–685.

Lees-Miller JP, Goodwin LO & Helfman DM (1990*a*). Three novel brain tropomyosin isoforms are expressed from the rat alpha-tropomyosin gene through the use of alternative promoters and alternative RNA processing. *Mol Cell Biol* **10**, 1729–1742.

Lees-Miller JP & Helfman DM (1991). The molecular basis for tropomyosin isoform diversity. *Bioessays* **13**, 429–437.

Lees-Miller JP, Yan A & Helfman DM (1990*b*). Structure and complete nucleotide sequence of the gene encoding rat fibroblast tropomyosin 4. *J Mol Biol* **213**, 399–405.

Lorenz M, Poole KJ, Popp D, Rosenbaum G & Holmes KC (1995). An atomic model of the unregulated thin filament obtained by X-ray fiber diffraction on oriented actin-tropomyosin gels. *J Mol Biol* **246**, 108–119.

McLachlan AD & Stewart M (1975). Tropomyosin coiled-coil interactions: evidence for an unstaggered structure. *J Mol Biol* **98**, 293–304.

McLachlan AD & Stewart M (1976). The 14-fold periodicity in alpha–tropomyosin and the interaction with actin. *J Mol Biol* **103**, 271–298.

McRee DE (1999). XtalView/Xfit – A versatile program for manipulating atomic coordinates and electron density. *J Struct Biol* **125**, 156–165.

Michele DE, Albayya FP & Metzger JM (1999). Direct, convergent hypersensitivity of calcium-activated force generation produced by hypertrophic cardiomyopathy mutant alpha-tropomyosins in adult cardiac myocytes. *Nat Med* **5**, 1413–1417.

Moraczewska J & Hitchcock-DeGregori SE (2000). Independent functions for the N- and C-termini in the overlap region of tropomyosin. *Biochemistry* **39**, 6891–6897.

Moraczewska J, Nicholson-Flynn K & Hitchcock-DeGregori SE (1999). The ends of tropomyosin are major determinants of actin affinity and myosin subfragment 1-induced binding to F-actin in the open state. *Biochemistry* **38**, 15885–15892.

Moss RL (1999). Plasticity in the dynamics of myocardial contraction: Ca^{2+}, crossbridge kinetics, or molecular cooperation. *Circ Res* **84**, 862–865.

Muthuchamy M, Boivin GP, Grupp IL & Wieczorek DF (1998). Beta-tropomyosin overexpression induces severe cardiac abnormalities. *J Mol Cellular Cardiol* **30**, 1545–1557.

Muthuchamy M, Grupp IL, Grupp G, O'Toole BA, Kier AB, Boivin GP, Neumann J & Wieczorek DF (1995). Molecular and physiological effects of overexpressing striated muscle beta-tropomyosin in the adult murine heart. *J Biol Chem* **270**, 30593–30603.

Muthuchamy M, Pajak L, Howles P, Doetschman T & Wieczorek DF (1993). Developmental analysis of tropomyosin gene expression in embryonic stem cells and mouse embryos. *Mol Cell Biol* **13**, 3311–3323.

Muthuchamy M, Pieples K, Rethinasamy P, Hoit B, Grupp IL, Boivin GP, Wolska B, Evans C, Solaro RJ & Wieczorek DF (1999). Mouse model of a familial hypertrophic cardiomyopathy mutation in alpha- tropomyosin manifests cardiac dysfunction. *Circ Res* **85**, 47–56.

Nicholls A, Sharp KA & Honig B (1991). Protein folding and association: insights from the interfacial and thermodynamic properties of hydrocarbons. *Proteins* **11**, 281–296.

Olson TM, Kishimoto NY, Whitby FG & Michels VV (2001). Mutations that alter the surface charge of alpha-tropomyosin are associated with dilated cardiomyopathy. *J Mol Cellular Cardiol* **33**, 723–732.

Pagani E & Solaro R (1984). Methods for measuring functional properties of sarcoplasmic reticulum and myofibrils in small samples of myocardium. In *Methods in Pharmacology*, ed.Schwartz A, pp. 49–61. Plenum Publishing Corp, New York.

Palmiter KA, Kitada Y, Muthuchamy M, Wieczorek DF & Solaro RJ (1996). Exchange of beta- for alpha-tropomyosin in hearts of transgenic mice induces changes in thin filament response to Ca^{2+}, strong cross-bridge binding, and protein phosphorylation. *J Biol Chem* **271**, 11611–11614.

Parry DA (1975). Analysis of the primary sequence of alpha-tropomyosin from rabbit skeletal muscle. *J Mol Biol* **98**, 519–535.

Paulucci AA, Hicks L, Machado A, Miranda MT, Kay CM & Farah CS (2002). Specific sequences determine the stability and cooperativity of folding of the C-terminal half of tropomyosin. *J Biol Chem* **277**, 39574–39584.

Pieples K & Wieczorek DF (2000). Tropomyosin 3 increases striated muscle isoform diversity. *Biochemistry* **39**, 8291–8297.

Prabhakar R, Boivin GP, Grupp IL, Hoit B, Arteaga G, Solaro JR & Wieczorek DF (2001). A familial hypertrophic cardiomyopathy alpha-tropomyosin mutation causes severe cardiac hypertrophy and death in mice. *J Mol Cellular Cardiol* **33**, 1815–1828.

Regitz-Zagrosek V, Erdmann J, Wellnhofer E, Raible J & Fleck E (2000). Novel mutation in the alpha-tropomyosin gene and transition from hypertrophic to hypocontractile dilated cardiomyopathy. *Circulation* **102**, E112–E116.

Ruiz-Opazo N & Nadal-Ginard B (1987). Alpha-tropomyosin gene organization. Alternative splicing of duplicated isotype-specific exons accounts for the production of smooth and striated muscle isoforms. *J Biol Chem* **262**, 4755–4765.

Schachat FH, Bronson DD & McDonald OB (1985). Heterogeneity of contractile proteins. A continuum of troponin-tropomyosin expression in mammalian skeletal muscle. *J Biol Chem* **260**, 1108–1113.

Schachat FH, Diamond MS & Brandt PW (1987). Effect of different troponin T-tropomyosin combinations on thin filament activation. *J Mol Biol* **198**, 551–554.

Smillie L (1996). Tropomyosin. In *Biochemistry of Smooth Muscle Contraction*, ed.Barany M, pp. 63–75. Academic Press, New York.

Squire JM & Morris EP (1998). A new look at thin filament regulation in vertebrate skeletal muscle. *Faseb J* **12**, 761–771.

Stewart M & McLachlan AD (1975). Fourteen actin-binding sites on tropomyosin? *Nature* **257**, 331–333.

Subramaniam A, Jones WK, Gulick J, Wert S, Neumann J & Robbins J (1991). Tissue-specific regulation of the alpha-myosin heavy chain gene promoter in transgenic mice. *J Biol Chem* **266**, 24613–24620.

Thierfelder L, MacRae C, Watkins H, Tomfohrde J, Williams M, McKenna W, Bohm K, Noeske G, Schlepper M, Bowcock A *et al.* (1993). A familial hypertrophic cardiomyopathy locus maps to chromosome 15q2. *Proc Natl Acad Sci U S A* **90**, 6270–6274.

Thierfelder L, Watkins H, MacRae C, Lamas R, McKenna W, Vosberg HP, Seidman JG & Seidman CE (1994). Alpha-tropomyosin and cardiac troponin T mutations cause familial hypertrophic cardiomyopathy: a disease of the sarcomere. *Cell* **77**, 701–712.

Thomas L & Smillie L (1994). Comparison of the interaction and functional properties of dephosphorylated hetero- and homo-dimers of rabbit striated muscle tropomyosins. *Biophysics J* **66**, A310, W-Pos 339.

Towbin H, Staehelin T & Gordon J (1979). Electrophoretic transfer of proteins from polyacrylamide gels to nitrocellulose sheets: procedure and some applications. *Proc Natl Acad Sci U S A* **76**, 4350–4354.

Walter CA, Nasr-Schirf D & Luna VJ (1989). Identification of transgenic mice carrying the CAT gene with PCR amplification. *Biotechniques* **7**, 1065–1070.

Whitby FG & Phillips GN Jr (2000). Crystal structure of tropomyosin at 7 Angstroms resolution. *Proteins* **38**, 49–59.

Wieczorek DF, Periasamy M, Butler-Browne GS, Whalen RG & Nadal-Ginard B (1985). Co-expression of multiple myosin heavy chain genes, in addition to a tissue-specific one, in extraocular musculature. *J Cell Biol* **101**, 618–629.

Wolska BM, Keller RS, Evans CC, Palmiter KA, Phillips RM, Muthuchamy M, Oehlenschlager J, Wieczorek DF, de Tombe PP & Solaro RJ (1999). Correlation between myofilament response to Ca^{2+} and altered dynamics of contraction and relaxation in transgenic cardiac cells that express beta-tropomyosin. *Circ Res* **84**, 745–751.